Article

Chinese Science Bulletin

SPECIAL ISSUE: New Energy Materials

November 2012 Vol.57 No.32: 4176–4180
doi: 10.1007/s11434-012-5248-2

Nonstoichiometric $Li_{1\pm x}Ni_{0.5}Mn_{1.5}O_4$ with different structures and electrochemical properties

FENG XuYong, SHEN Chen, FANG Xin & CHEN ChunHua*

CAS Key Laboratory of Materials for Energy Conversions, Department of Materials Science and Engineering, University of Science and Technology of China, Hefei 230026, China

Received September 22, 2011; accepted November 23, 2011; published online June 8, 2012

$Li_{1\pm x}Ni_{0.5}Mn_{1.5}O_4$ (x=0.05, 0) spinel powders were synthesized using a solid-state reaction. Their structures were characterized by X-ray diffraction, scanning electron microscopy and Raman spectroscopy. Their electrochemical properties for use as active cathode materials in lithium-ion batteries were measured. The $LiNi_{0.5}Mn_{1.5}O_4$, $Li_{1.05}Ni_{0.5}Mn_{1.5}O_4$ and $Li_{0.95}Ni_{0.5}Mn_{1.5}O_4$ samples crystallized in $Fd\bar{3}m$, $Fd\bar{3}m$ and $P4_332$, respectively. The $LiNi_{0.5}Mn_{1.5}O_4$ and $Li_{0.95}Ni_{0.5}Mn_{1.5}O_4$ samples exhibited better cycle performance than the $Li_{1.05}Ni_{0.5}Mn_{1.5}O_4$ sample, while $Li_{0.95}Ni_{0.5}Mn_{1.5}O_4$ had the worst rate performance. Thus, it appears unnecessary to introduce nominal lithium nonstoichiometry in $LiNi_{0.5}Mn_{1.5}O_4$ electrode materials.

lithium nickel manganese oxide, space group, Raman spectroscopy, cyclic voltammetry, cycle performance, rate capability

Citation: Feng X Y, Shen C, Fang X, et al. Nonstoichiometric $Li_{1\pm x}Ni_{0.5}Mn_{1.5}O_4$ with different structures and electrochemical properties. Chin Sci Bull, 2012, 57: 4176–4180, doi: 10.1007/s11434-012-5248-2

High energy lithium-ion batteries are in increasing demand for many applications including hybrid vehicles. As the energy of a cell is the voltage multiplied by its capacity, there are two ways to improve the energy density; i.e. either the voltage or the capacity can be increased. $LiNi_{0.5}Mn_{1.5}O_4$ spinel exhibits a voltage of about 4.7 V [1–4], which is higher than other electrode materials like $LiMn_2O_4$ (4 V [5]), $LiCoO_2$ (4 V [6]) and $LiFePO_4$ (3.4 V [7]). In the past decade, many methods have been used to synthesize this high voltage material, including solid-state reactions [8–10], sol-gel processes [11,12], and co-precipitation [13,14]. The properties of the synthesized $LiNi_{0.5}Mn_{1.5}O_4$ samples are strongly influenced by the synthetic method. Samples typically contain $Li_xNi_{1-x}O_2$ as an impurity in the products, especially those produced by solid-state methods [8–10], and this secondary phase is formed because of oxygen loss at high temperatures. In addition, the oxygen loss reaction results in the generation of Mn^{3+} ions which can further deteriorate the electrochemical performance.

$LiNi_{0.5}Mn_{1.5}O_4$ occurs in two different space groups, $Fd\bar{3}m$ and $P4_332$. Specifically, the nonstoichiometric $LiNi_{0.5}Mn_{1.5}O_{4-x}$ and stoichiometric $LiNi_{0.5}Mn_{1.5}O_4$ occupy the $Fd\bar{3}m$ and $P4_332$ phases, respectively [15]. The oxygen-deficient composition $LiNi_{0.5}Mn_{1.5}O_{4-x}$ is stable at temperatures over 800°C, but, when annealed at 700°C, the symmetry changes to $P4_332$. The $Fd\bar{3}m$ phase has a lower impedance and hence higher capacity at high rates. In addition, the cycle performance of the $P4_332$ phase is worse than that of the $Fd\bar{3}m$ phase because it must form an intermediate $Fd\bar{3}m$ phase during Li extraction. In addition to the annealing process, the synthetic method can also influence the space group of the $LiNi_{0.5}Mn_{1.5}O_4$ products [16,17].

1 Experimental

The spinel $Li_{1\pm x}Ni_{0.5}Mn_{1.5}O_4$ (x=0, 0.05) samples were synthesized via a two-step solid state reaction process [18]. All chemicals were purchased from Sinopharm Chemical Rea-

*Corresponding author (email: cchchen@ustc.edu.cn)

gent Co., Ltd. Nickel acetate ($Ni(Ac)_2{\cdot}4H_2O$, 10 mmol) and manganese acetate ($Mn(Ac)_2{\cdot}4H_2O$, 30 mmol) were first mixed and ground in a mortar and then calcined in air at a rate of 3°C min^{-1} in an alumina crucible to 500°C. The sample was held at 500°C for 5 h followed by natural cooling to room temperature. To determine how much $LiAc{\cdot}2H_2O$ should be added, the mass of the sample was determined before calcination (9.3535 g) and after (2.9891 g). Thus, 31.96% of the mass remained, meaning 0.7863 g of the residual oxides corresponded to 2.5 mmol $Ni(Ac)_2{\cdot}4H_2O$ and 7.5 mmol $Mn(Ac)_2{\cdot}4H_2O$ in the starting mixture. Next, 0.7863 g of the Ni-Mn oxide was mixed with 0.5356 g (5.25 mmol), 0.501 g (5 mmol), 0.4846 g (4.75 mmol) of $LiAc{\cdot}2H_2O$, to obtain the $Li_{1.05}Ni_{0.5}Mn_{1.5}O_4$, $LiNi_{0.5}Mn_{1.5}O_4$, and $Li_{0.95}Ni_{0.5}Mn_{1.5}O_4$ powders, respectively. These samples were first calcined at 500°C for 5 h, and then sintered at 900°C for 10 h, cooled to 700°C, and annealed for 10 h.

The crystalline structures of the $Li_{1\pm x}Ni_{0.5}Mn_{1.5}O_4$ (x=0, 0.05) samples were characterized by X-ray diffraction (XRD, Rigaku TTR-III, CuKα radiation). The diffraction patterns were recorded at room temperature over the 2θ range from 10° to 80°. Raman spectra of these samples were measured on a LABRAM-HR Confocal Laser Micro-Raman spectrometer using an argon laser (wavelength 514.5 nm) at room temperature. The morphology and particle size were characterized by scanning electron microscopy (JSM-6390LA, JEOL).

The electrochemical properties of $Li_{1\pm x}Ni_{0.5}Mn_{1.5}O_4$ (x=0, 0.05) were measured in CR2032 coin-type half-cells using lithium metal as a negative electrode. The positive electrodes consisted of a mixture of 84 wt% $Li_{1\pm x}Ni_{0.5}Mn_{1.5}O_4$ (x=0, 0.05) samples, 8 wt% carbon black and 8 wt% PVDF binder. The cells were assembled in an argon-filled dry-box (MBraun Labmaster 130) with a porous polypropylene membrane (Celgard 2400) as the separator and 1 mol/L $LiPF_6$ in EC:DMC (1:1; v/v) as the electrolyte. These half-cells were cycled on a multi-channel battery test system (NEWARE BTS-610) over the voltage range from 3.5 to 5.1 V. Cyclic voltammograms (CV) were measured on a CHI 604 Electrochemical Workstation with a scanning rate of 0.2 mV s^{-1} from 3.5 to 5.1 V.

2 Results and discussion

2.1 Structure and morphology of $Li_{1\pm x}Ni_{0.5}Mn_{1.5}O_4$

The X-ray diffraction patterns of the prepared $Li_{1\pm x}Ni_{0.5}Mn_{1.5}O_4$ (x=0, 0.05) samples are shown in Figure 1, all of which exhibit the cubic spinel structure of $LiNi_{0.5}Mn_{1.5}O_4$ (Figure 1(a)). In the $LiNi_{0.5}Mn_{1.5}O_4$, there are two additional peaks at 37° and 45° that correspond to an impurity phase of $Li_xNi_{1-x}O_2$, suggesting an oxygen loss reaction at high temperatures. Also, the positions of the diffraction peaks of nominal $Li_{1.05}Ni_{0.5}Mn_{1.5}O_4$ and $Li_{0.95}Ni_{0.5}Mn_{1.5}O_4$ shift to the higher angles than $Li_{1.00}Ni_{0.5}Mn_{1.5}O_4$ (Figure 1(b)), meaning the lattice parameters of the $Li_{1\pm0.05}Ni_{0.5}Mn_{1.5}O_4$ samples are smaller than the $LiNi_{0.5}Mn_{1.5}O_4$ sample. In the sample with the nominal composition of "$Li_{1.05}Ni_{0.5}Mn_{1.5}O_4$", some lithium ions must be in Ni or Mn sites, resulting in a higher concentration of Mn^{4+} ions compared to the stoichiometric $Li_{1.0}Ni_{0.5}Mn_{1.5}O_4$ sample. Mn^{4+} has stronger electrostatic interactions than Mn^{3+} which leads to smaller lattice parameters. On the other hand, for the sample with the nominal composition of "$Li_{0.95}Ni_{0.5}Mn_{1.5}O_4$", some Ni^{2+} ions occupy Li^+ site to form a $[Li_{0.97}Ni_{0.03}][Ni_{0.48}Mn_{1.52}]O_4$ phase. Because Ni^{2+} has a similar radius (0.78 Å, Goldschmidt radius) to Li^+ but with a higher charge, the stronger electrostatic interaction also results in smaller lattice parameters.

The fine structure of a crystal can be also characterized by Raman spectroscopy. As seen in Figure 2, $LiNi_{0.5}Mn_{1.5}O_4$ and $Li_{1.05}Ni_{0.5}Mn_{1.5}O_4$ samples have the same Raman spectrum, which can be assigned to the $Fd\bar{3}m$ space group [17,19]. The $Li_{0.95}Ni_{0.5}Mn_{1.5}O_4$ sample has two peaks at 218 and 240 cm^{-1} that are attributed to the $P4_332$ space group, and has been assigned as such.

In addition, the sample $Li_{0.90}Ni_{0.5}Mn_{1.5}O_4$ was synthesized and characterized by Raman spectrum to ensure the symmetry change of samples lack of lithium. As discussed above, $Li_{0.95}Ni_{0.5}Mn_{1.5}O_4$ can be written as $[Li_{0.97}Ni_{0.03}][Ni_{0.48}Mn_{1.52}]O_4$ giving an average valence of the manganese a little less than +4.

The scanning electron microscopy images of these samples are shown in Figure 3. No obvious impurity phase can

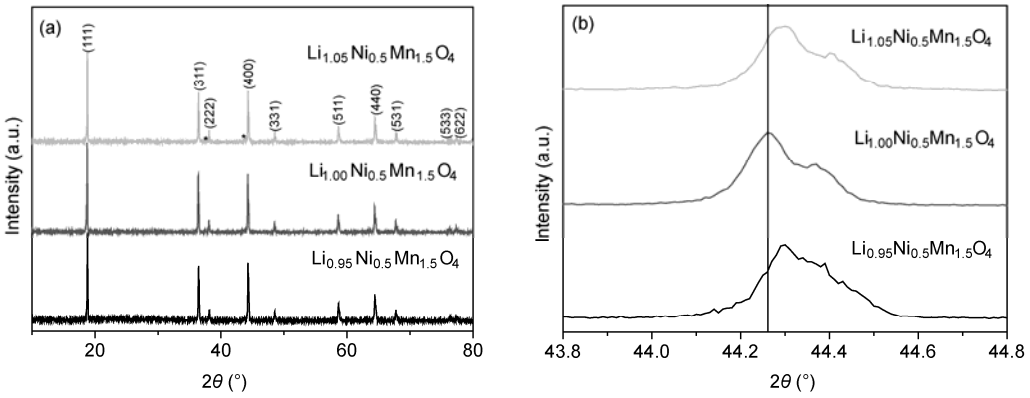

Figure 1 XRD patterns of the $Li_{1\pm x}Ni_{0.5}Mn_{1.5}O_4$ samples. (a) Full patterns; (b) enlargement of the (111) peaks.

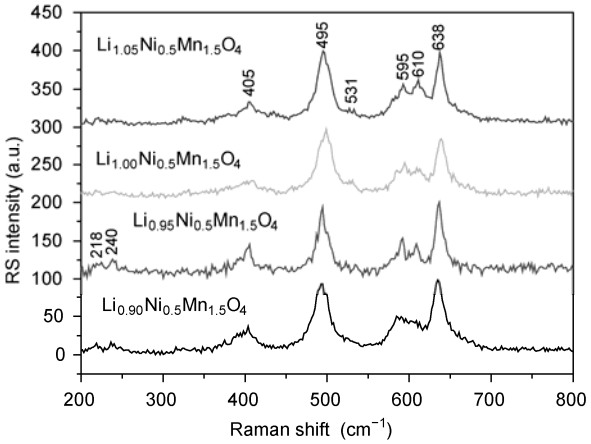

Figure 2 Raman spectra of the $Li_{1\pm x}Ni_{0.5}Mn_{1.5}O_4$ samples.

be seen. The particle sizes of the $Li_{0.95}Ni_{0.5}Mn_{1.5}O_4$ and $Li_{1.05}Ni_{0.5}Mn_{1.5}O_4$ samples are almost in the same range of 2–4 μm, which are obviously bigger than the $LiNi_{0.5}Mn_{1.5}O_4$ sample with an average particle size around 1 μm. Apparently, the nonstoichiometries of these spinel materials, with either excessive or deficient lithium, facilitate the growth of particles during the solid state reaction.

2.2 Electrochemical performance of $Li_{1\pm x}Ni_{0.5}Mn_{1.5}O_4$

The galvanostatic charge-discharge curves (4th cycle) of the $Li_{1\pm x}Ni_{0.5}Mn_{1.5}O_4$ electrodes at a current density of 150 mA g^{-1} are shown in Figure 4. The specific capacities of these three samples are similar. Their differences are seen between 3.5 and 4.5 V, which corresponds to the conversion of Mn^{4+} to Mn^{3+}. The higher the concentration of lithium is, the lower the specific capacity between 3.5 and 4.5 V. This means the concentration of Mn^{3+} ions increases with a reduction in the quantity of lithium ions. It is also seen in Figure 4 that the discharge voltage of these samples decreases with the cycle number. The change in voltage relates to an increase in the impedance that comes from the decomposition of the electrolyte and the formation of a surface film on the

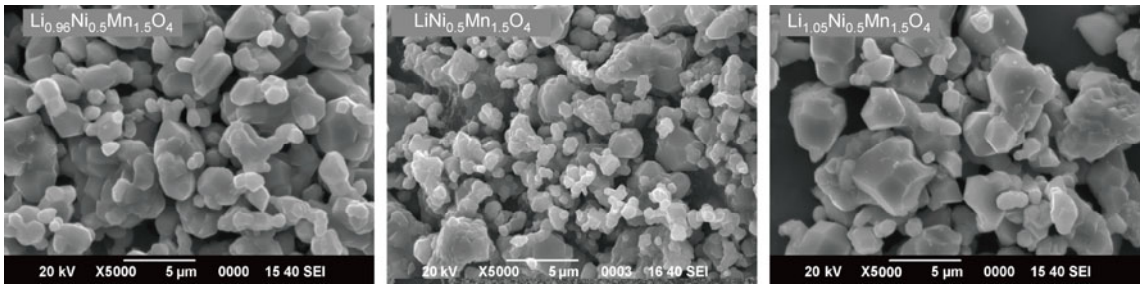

Figure 3 SEM images of the $Li_{1\pm x}Ni_{0.5}Mn_{1.5}O_4$ samples.

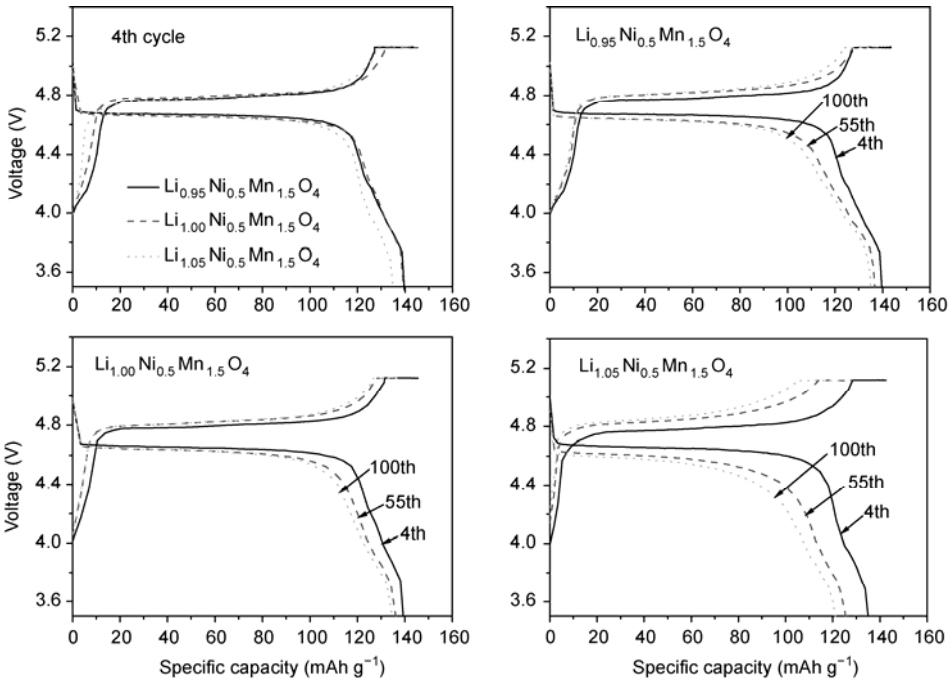

Figure 4 Voltage profiles of the $Li_{1\pm x}Ni_{0.5}Mn_{1.5}O_4$/Li cells at a current density of 150 mA g^{-1}.

particles. Among the three samples, the $Li_{1.05}Ni_{0.5}Mn_{1.5}O_4$ electrode gave the largest change in volt-age, which may be due to the high valence manganese making it easier to oxidize the electrolyte and make the surface films thicker and more resistive.

Figure 5 shows the cycle performance of the $Li_{1\pm x}Ni_{0.5}Mn_{1.5}O_4$ electrodes. $Li_{0.95}Ni_{0.5}Mn_{1.5}O_4$ has a good cycle performance that retains about 96% of its initial capacity after 100 cycles, with only 0.05 mAh g^{-1} capacity loss per cycle. This may be due to the smaller lattice parameters seen in the XRD patterns mentioned earlier making the sample more stable. $LiNi_{0.5}Mn_{1.5}O_4$ (Figure 5) has almost the same excellent cycle performance (96.6% capacity retained after 100 cycles, Figure 5). The worst is the $Li_{1.05}Ni_{0.5}Mn_{1.5}O_4$ electrode, which has a smaller lattice parameter than $Li_{0.95}Ni_{0.5}Mn_{1.5}O_4$ and also contains less Mn^{3+}. From Figure 4 we can attribute this capacity fading to the increase in impedance during the cycling.

Cyclic voltammetry curves the $Li/Li_{1\pm x}Ni_{0.5}Mn_{1.5}O_4$ half-cells are shown in Figure 6. These samples have two peaks at 4.0 and 4.7 V in the discharge process. As mentioned before, the peak at 4.7 V refers to the 4.7 V plateau in the Galvanostatic discharge curves and peak at 4.0 V to the sloping portion between 3.5 and 4.5 V (Figure 4). The voltage difference between the charge curve and discharge curve is related to the impedance of the cells. Thus, once again, the voltage difference of the $Li/Li_{0.95}Ni_{0.5}Mn_{1.5}O_4$ cell is the largest of all the cells, and this is due to the change in the space group.

The rate performances of the $Li_{1\pm x}Ni_{0.5}Mn_{1.5}O_4$ electrodes are presented in Figure 7. At 1 C, the $Li_{0.95}Ni_{0.5}Mn_{1.5}O_4$ electrode delivers the highest capacity, the $LiNi_{0.5}Mn_{1.5}O_4$ electrode the second, and the $Li_{1.05}Ni_{0.5}Mn_{1.5}O_4$ electrode the lowest. But when the rate increases to 3 C, the capacity of the $LiNi_{0.5}Mn_{1.5}O_4$ electrode becomes higher than $Li_{0.95}Ni_{0.5}Mn_{1.5}O_4$ because of the lower impedance. When the rate is increased to 10 C, the $Li_{0.95}Ni_{0.5}Mn_{1.5}O_4$ electrode can only retain 66% of the capacity at 1 C. The $LiNi_{0.5}Mn_{1.5}O_4$ electrode shows the best electrochemical performance because of its better cycle performance and higher capacity than $Li_{1.05}Ni_{0.5}Mn_{1.5}O_4$, and lower impedance than $Li_{0.95}Ni_{0.5}Mn_{1.5}O_4$. It can retain a capacity of about 113 mAh g^{-1} at the rate of 10 C, 82% of its capacity at 1 C, which is better than that reported in literature [20,21]. The rate performance of $Li_{1.05}Ni_{0.5}Mn_{1.5}O_4$ is between the other two samples in that its capacity at 10 C is about 104 mAh g^{-1}, or 77% of that at 1 C.

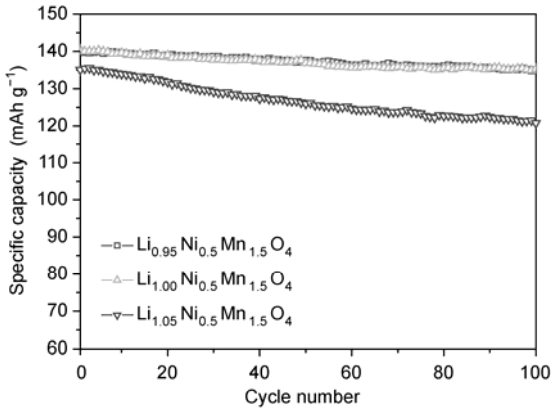

Figure 5 Cycle performance of the $Li_{1\pm x}Ni_{0.5}Mn_{1.5}O_4$/Li cells at a current density of 150 mA g^{-1}.

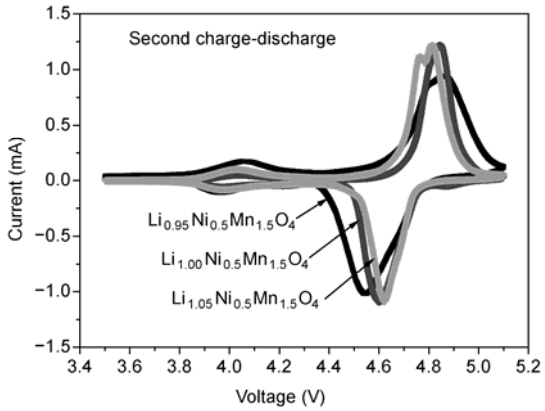

Figure 6 Cyclic voltammograms of the $Li_{1\pm x}Ni_{0.5}Mn_{1.5}O_4$/Li cells in the second cycle at a rate of 0.2 mV s^{-1}.

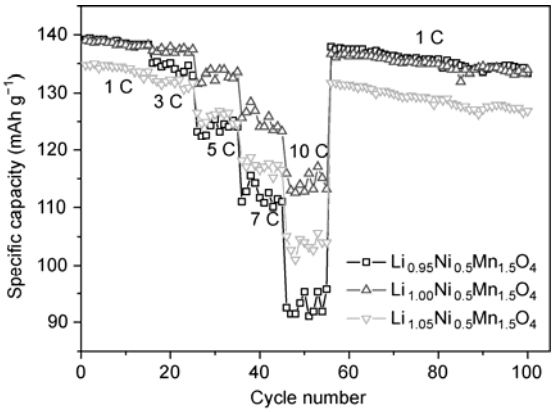

Figure 7 Rate performance of the $Li_{1\pm x}Ni_{0.5}Mn_{1.5}O_4$ samples.

3 Conclusions

Nonstoichiometric $Li_{1\pm x}Ni_{0.5}Mn_{1.5}O_4$ (x=0, 0.05) spinel powders have been synthesized by a solid-state reaction. The $Li_{0.95}Ni_{0.5}Mn_{1.5}O_4$ sample has good cycle performance because of a smaller lattice parameter and better crystal stability, but the lack of lithium leads to a phase conversion from $Fd\bar{3}m$ to $P4_332$ with higher impedance, and hence the worst rate performance. The $Li_{1.05}Ni_{0.5}Mn_{1.5}O_4$ sample delivers the lowest specific capacity and worst cycle performance. Therefore, it is unnecessary to introduce lithium nonstoichiometry into $LiNi_{0.5}Mn_{1.5}O_4$ electrode materials. The nominal stoichiometric $LiNi_{0.5}Mn_{1.5}O_4$ electrode gives the best cycle and rate performances.

This work was supported by the National Natural Science Foundation of China (20971117 and 10979049) and the Education Department of Anhui Province (KJ2009A142). We are also grateful to the Solar Energy Operation Plan of Academia Sinica.

1 Lee Y S, Sun Y K, Ota S, et al. Preparation and characterization of nano-crystalline $LiNi_{0.5}Mn_{1.5}O_4$ for 5 V cathode material by composite carbonate process. Electrochem Commun, 2002, 4: 989–994
2 Lazarraga M G, Pascual L, Gadjov H, et al. Nanosize $LiNi_yMn_{2-y}O_4$ ($0<y\leqslant 0.5$) spinels synthesized by a sucrose-aided combustion method. Characterization and electrochemical performance. J Mat Chem, 2004, 14: 1640–1647
3 Markevich E, Baranchugov V, Aurbach D. On the possibility of using ionic liquids as electrolyte solutions for rechargeable 5 V Li ion batteries. Electrochem Commun, 2006, 8: 1331–1334
4 Xu H Y, Xie S, Ding N, et al. Improvement of electrochemical properties of $LiNi_{0.5}Mn_{1.5}O_4$ spinel prepared by radiated polymer gel method. Electrochim Acta, 2006, 51: 4352–4357
5 Lee H W, Muralidharan P, Ruffo R, et al. Ultrathin spinel $LiMn_2O_4$ nanowires as high power cathode materials for Li-ion batteries. Nano Lett, 2010, 10: 3852–3856
6 Zhuang Q C, Xu J M, Fan X Y, et al. An electrochemical impedance spectroscopic study of the electronic and ionic transport properties of $LiCoO_2$ cathode. Chin Sci Bull, 2007, 52: 187–1195
7 Deng F, Zeng X R, Zou J Z, et al. Synthesis of $LiFePO_4$ *in situ* vapor-grown carbon fiber (VGCF) composite cathode material via microwave pyrolysis chemical vapor deposition. Chin Sci Bull, 2011, 56: 832–835
8 Santhanam R, Rambabu B. Research progress in high voltage spinel $LiNi_{0.5}Mn_{1.5}O_4$ material. J Power Sources, 2010, 195: 5442–5451
9 Chi L H, Dinh N N, Brutti S, et al. Synthesis, characterization and electrochemical properties of 4.8 V $LiNi_{0.5}Mn_{1.5}O_4$ cathode material in lithium-ion batteries. Electrochim Acta, 2010, 55: 5110–5116
10 Chen Z Y, Zhu H L, Ji S, et al. Performance of $LiNi_{0.5}Mn_{1.5}O_4$ prepared by solid-state reaction. J Power Sources, 2009, 189: 507–510
11 Du G D, NuLi Y, Yang J, et al. Fluorine-doped $LiNi_{0.5}Mn_{1.5}O_4$ for 5 V cathode materials of lithium-ion battery. Mater Res Bull, 2008, 43: 3607–3613
12 Yang T Y, Sun K N, Lei Z Y, et al. The influence of holding time on the performance of $LiNi_{0.5}Mn_{1.5}O_4$ cathode for lithium ion battery. J Alloys Compd, 2010, 502: 215–219
13 Zhang X F, Liu J, Yu H Y, et al. Enhanced electrochemical performances of $LiNi_{0.5}Mn_{1.5}O_4$ spinel via ethylene glycol-assisted synthesis. Electrochim Acta, 2010, 55: 2414–2417
14 Liu J, Manthiram A. Understanding the improved electrochemical performances of Fe-substituted 5 V spinel cathode $LiMn_{1.5}Ni_{0.5}O_4$. J Phys Chem C, 2009, 113: 15073–15079
15 Kim J H, Myung S T, Yoon C S, et al. Comparative study of $LiNi_{0.5}Mn_{1.5}O_{4-x}$ and $LiNi_{0.5}Mn_{1.5}O_4$ cathodes having two crystallographic structures: Fd-3m and $P4_332$. Chem Mater, 2004, 16: 906–914
16 Fang H S, Li L P, Li G S. A low-temperature reaction route to high rate and high capacity $LiNi_{0.5}Mn_{1.5}O_4$. J Power Sources, 2007, 167: 223–227
17 Amdouni N, Zaghib K, Gendron F. Structure and insertion properties of disordered and ordered $LiNi_{0.5}Mn_{1.5}O_4$ spinels prepared by wet chemistry. Ionics, 2006, 12: 117–126
18 Feng X Y, Shen C, Fang X, et al. Synthesis of $LiNi_{0.5}Mn_{1.5}O_4$ by solid-state reaction with improved electrochemical performance. J Alloys Compd, 2011, 509: 3623–3626
19 Julien C M, Gendron F, Amdouni A, et al. Lattice vibrations of materials for lithium rechargeable batteries. VI: Ordered spinels. Mater Sci Eng B, 2006, 130: 41–48
20 Li D C, Ito A, Kobayakawa K, et al. Electrochemical characteristics of $LiNi_{0.5}Mn_{1.5}O_4$ prepared by spray drying and post-annealing. Electrochim Acta, 2007, 52: 1919–1924
21 Yi T F, Hu X G. Preparation and characterization of sub-micro $LiNi_{0.5-x}Mn_{1.5+x}O_4$ for 5 V cathode materials synthesized by an ultrasonic-assisted co-precipitation method. J Power Sources, 2007, 167: 185–191